HHS Public Access

Author manuscript

J Comp Neurol. Author manuscript; available in PMC 2016 May 01.

Published in final edited form as:

J Comp Neurol. 2015 May 1; 523(7): 1038–1053. doi:10.1002/cne.23706.

Connectivity of Pacemaker Neurons in the Neonatal Rat Superficial Dorsal Horn

Jie Li[#1], **Elizabeth Kritzer**[#1], **Neil C. Ford**[1,2], **Shahriar Arbabi**[1], and **Mark L. Baccei**[1,2]

[1]Pain Research Center, Dept. of Anesthesiology, University of Cincinnati Medical Center, 231 Albert Sabin Way, Cincinnati OH 45267

[2]Neuroscience Graduate Program, University of Cincinnati, Cincinnati OH 45267

[#] These authors contributed equally to this work.

Abstract

Pacemaker neurons with an intrinsic ability to generate rhythmic burst-firing have been characterized in lamina I of the neonatal spinal cord, where they are innervated by high-threshold sensory afferents. However, little is known about the output of these pacemakers, as the neuronal populations which are targeted by pacemaker axons have yet to be identified. The present study combines patch clamp recordings in the intact neonatal rat spinal cord with tract-tracing to demonstrate that lamina I pacemaker neurons contact multiple spinal motor pathways during early life. Retrograde labeling of premotor interneurons with the trans-synaptic virus PRV-152 revealed the presence of burst-firing in PRV-infected lamina I neurons, thereby confirming that pacemakers are synaptically coupled to motor networks in the spinal ventral horn. Notably, two classes of pacemakers could be distinguished in lamina I based on cell size and the pattern of their axonal projections. While small pacemaker neurons possessed ramified axons which contacted ipsilateral motor circuits, large pacemaker neurons had unbranched axons which crossed the midline and ascended rostrally in the contralateral white matter. Recordings from identified spino-parabrachial and spino-PAG neurons indicated the presence of pacemaker activity within neonatal lamina I projection neurons. Overall, these results show that lamina I pacemakers are positioned to regulate both the level of activity in developing motor circuits as well as the ascending flow of nociceptive information to the brain, thus highlighting a potential role for pacemaker activity in the maturation of pain and sensorimotor networks in the CNS.

Keywords

spinal cord; burst-firing; lamina I; premotor interneuron; synapse; AB_2336883; AB_2301751; AB_1587626

Corresponding Author: Mark L. Baccei, Ph.D., Pain Research Center, Dept. of Anesthesiology, University of Cincinnati Medical Center, 231 Albert Sabin Way, Cincinnati, OH 45267; Ph: 1-513-558-5037; FAX: 1-513-558-0995; mark.baccei@uc.edu.

Role of authors: All authors had full access to all the data in the study and take responsibility for the integrity of the data and the accuracy of the data analysis. Study concept and design: JL, EK, MB. Acquisition of data: JL, EK, NF, SA, MB. Analysis and interpretation of data: JL, EK, NF, SA, MB. Drafting of the manuscript: JL, EK, MB. Critical revision of the manuscript for important intellectual content: JL, EK, NF, MB. Statistical analysis: EK, MB. Obtained funding: MB. Administrative, technical, and material support: EK. Study supervision: MB.

Conflict of Interest Statement: The authors declare no competing financial interests.

Introduction

Pacemaker neurons exhibiting intrinsic burst-firing serve as important drivers of spontaneous activity within many developing networks of the CNS (Sipila et al., 2005; Zheng et al., 2006; Lischalk et al., 2009), including the ventral horn of the spinal cord (Tazerart et al., 2007; Tazerart et al., 2008). Recently, we have also characterized pacemakers within the superficial dorsal horn (SDH) (Li and Baccei, 2011), a region where nociceptive signals undergo extensive processing before being transmitted to the brain via the activity of ascending projection neurons (Todd, 2010). Using patch clamp recordings from spinal cord slices, we demonstrated that rhythmic burst-firing was restricted to lamina I in the immature SDH, down-regulated after the first postnatal week (Li and Baccei, 2011) and strongly modulated by the activation of inward-rectifying K^+ channels (Li et al., 2013). In addition, pacemakers were identified as a population of small glutamatergic interneurons (Li and Baccei, 2011), thus raising the possibility that they provide an endogenous source of excitation to developing spinal cord circuits.

Unfortunately, the functional significance of such pacemaker activity in lamina I remains unknown, in part because little is understood about the connectivity of these pacemaker neurons within the CNS. For example, rhythmic burst-firing in the SDH could facilitate the initiation of spontaneous muscle contractions that commonly occur in the neonatal rodent and are known to be partially generated by mechanisms intrinsic to the spinal cord (Blumberg and Lucas, 1994; Petersson et al., 2003; Waldenstrom et al., 2009). These contractions are thought to be essential to the generation of tactile sensory input required for the normal maturation of the spinal sensorimotor networks underlying the nociceptive withdrawal reflex (Waldenstrom et al., 2003). However, it is unclear if lamina I pacemaker neurons are synaptically connected to the motor pathways of the neonatal spinal cord. Similarly, rhythmic burst-firing in lamina I could potentially serve to synchronize the activity of nearby projection neurons, as has been reported in the auditory system (Tritsch et al., 2010), but it has yet to be shown that pacemakers innervate these output neurons of the SDH network. While previous work using the spinal cord slice preparation suggests that lamina I pacemakers project throughout the dorsal-ventral axis (Li and Baccei, 2011), their axons could not be followed to their final destination since they usually exited the plane of the slice. As a result, the specific CNS neuronal populations targeted by lamina I pacemaker neurons remain unknown.

Using recently described infrared imaging approaches which permit patch clamp recordings from SDH neurons within the intact spinal cord (Safronov et al., 2007; Szucs et al., 2009), in conjunction with tract-tracing techniques, the current study investigates the connectivity of lamina I pacemaker neurons during early life.

Materials and Methods

All experiments adhered to animal welfare guidelines established by the University of Cincinnati Institutional Animal Care and Use Committee.

Intact spinal cord preparation

Tissue preparation was performed as previously described (Li et al., 2013). Sprague-Dawley rat pups (P1-P5; n = 107 across all experiments) of either sex were terminally anesthetized with sodium pentobarbital (Fatal-Plus; Vortec Pharmaceuticals; Dearborn MI), transcardially perfused with oxygenated artificial cerebrospinal fluid (aCSF; composition in mM: 125 NaCl, 2.5 KCl, 25 $NaHCO_3$, 1.0 NaH_2PO_4, 1.0 $MgCl_2$, 2.0 $CaCl_2$, and 25 glucose, pH 7.2) and decapitated. The lumbar spinal cord was quickly removed, immersed in oxygenated aCSF and stripped of dura and pia mater on the dorsal surface. The intact spinal cord was placed in a submersion-type recording chamber (RC-22; Warner Instruments, Hamden, CT), mounted on the stage of an upright microscope (BX51WI; Olympus, Center Valley, PA) and perfused at room temperature (RT) with oxygenated aCSF at a rate of 1.5-3 ml/min.

Patch clamp recordings

Patch electrodes were constructed from thin-walled single-filamented borosilicate glass (1.5 mm outer diameter; World Precision Instruments, Sarasota FL) using a microelectrode puller (P-97; Sutter Instruments, Novato, CA). Pipette resistances ranged from 4 to 6 MΩ and seal resistances were >1 GΩ. Patch electrodes were filled with a solution containing the following (in mM): 130 K-gluconate, 10 KCl, 10 HEPES, 10 Na-phosphocreatine, 4 MgATP, and 0.3 Na_2-GTP, pH 7.2 (295-300 mOsm) with 0.3% biocytin added.

Lamina I neurons were visualized within the intact spinal cord using infrared LED illumination as described previously (Safronov et al., 2007; Szucs et al., 2009), and patch clamp recordings were obtained using a Multiclamp 700B amplifier (Molecular Devices, Sunnyvale, CA). Approximately 1 min after establishment of the whole-cell configuration, the spontaneous firing patterns of dorsal horn neurons were classified at the resting membrane potential (V_{rest}) as ‘silent’, ‘irregular’, ‘tonic’ or ‘bursting’ (Li and Baccei, 2011). Membrane capacitance was calculated using the built-in pClamp membrane test. Neurons which failed to exhibit rhythmic burst-firing (i.e. non-pacemakers) were immediately removed from the spinal cord under visual control via strong negative pressure applied to the electrode, thus ensuring that cells later identified with biocytin staining corresponded to pacemakers. Neurons exhibiting rhythmic burst-firing were dialyzed with biocytin for 30-40 min. Approximately 1-3 pacemakers per spinal cord were labeled in this manner across the L3-L5 region.

Biocytin staining and immunohistochemistry

Following the patch clamp recording, intact spinal cords were immersion-fixed in 4% paraformaldehyde in PBS overnight, then cryoprotected in 30% sucrose in PBS for another 24 hours. Cryoprotected spinal cords were embedded in Tissue Freezing Medium (General Data; Durham, NC) and rapidly frozen in a bath of isopentane cooled by dry ice. Frozen cords were stored at −80°C until they were sectioned on a Leica 1850CM cryostat. Transverse or parasagittal sections (20 μm) were serially collected on Superfrost slides (Fisher Scientific; Pittsburgh, PA) and allowed to dry at RT for at least 1 hour. Slides were stored at −20°C until use.

To visualize the morphology of biocytin-filled pacemaker neurons in the neonatal SDH, slides were rinsed 3 × 10 min with 0.01M PBS, followed by permeabilization with PBS + 0.3% Triton X-100 (PBS-Tx) for 30 min at RT. Sections were then blocked with PBS-Tx containing 10% normal goat serum (NGS) (S-1000; Vector Labs, Burlingame CA) for 1 hour at RT. Sections were incubated with Avidin-rhodamine or Avidin-AlexaFluor 488 conjugate (A3678 or A21370, respectively; Invitrogen, Carlsbad, CA) diluted at 1:1000 in 3% NGS in PBS-Tx for 3 hours at RT. Slides were washed 3 × 10 min in PBS then coverslipped with Vectashield mounting medium (H-1000; Vector Labs; Burlingame, CA).

For experiments involving the immunohistochemical analysis of pacemaker neurons and their potential targets, following the above blocking step, sections were incubated overnight at 4°C in primary antibodies raised against VGLUT2 (AB_1587626), VGLUT1 (AB_2301751) or GFP (AB_2336883; Table 1) diluted in 3% NGS in PBS-Tx. Sections were washed 3 × 10 min with PBS-Tx and incubated for 1 hr at RT in species-specific secondary antibodies (Table 1) diluted at 1:1000 in 3% NGS in PBS-Tx. Sections were then washed 3 × 10 min with PBS-Tx before proceeding with the visualization of the biocytin as described above.

Antibody Characterization

Anti-GFP polyclonal antibody stains a single band of 30 kDa on Western blot prepared from HeLa cell lysates expressing GFP. This band is absent in lanes on the same blot which contain lysate from control (i.e., non-GFP expressing) HeLa cells (manufacturer's technical information.) Staining frozen sections of naïve rat lumbar spinal cord produced no detectable immunoreactivity.

Anti-VGLUT1 polyclonal antibody recognizes a single band of 62 kDa on Western blot of protein prepared from rat brain lysate (manufacturer's technical information). Manufacturer reports staining of tissue sections from rat CNS is consistent with other antisera to VGLUT1. Staining frozen sections of rat lumbar spinal cord showed immunoreactivity patterns consistent with previous descriptions using a different VGLUT1 antibody (Landry et al. 2004).

Anti-VGLUT2 polyclonal antibody recognizes a 52 kDa band on Western blot of protein prepared from rat brain lysate (manufacturer's technical information). Staining frozen sections of rat lumbar spinal cord showed immunoreactivity patterns consistent with previous descriptions using a different VGLUT2 antibody (Landry et al. 2004).

DiI injections

Sprague Dawley rat pups of either sex (n = 8) were anesthetized with a mixture of ketamine (90 mg/kg) and xylazine (10 mg/kg) on postnatal day 0 (P0) to P1 and placed in a plaster body mold that was secured in a stereotaxic apparatus (World Precision Instruments) as described previously (Hoorneman, 1985). The scalp was incised and a small hole was made in the skull using an OmniDrill35 (World Precision Instruments, Sarasota, FL). The pup received a single injection (50–100 nl) of FAST DiI oil (2.5 mg/ml; Invitrogen) into either the parabrachial nucleus (PB) or the periaqueductal gray (PAG) using a Hamilton microsyringe (62RN; 2.5 μl volume) equipped with a 28 gauge needle. Following a series of

pilot experiments based on an atlas of the E22 (i.e., P0) rat brain by Altman and Bayer (1995), the following stereotaxic coordinates were used (in mm; relative to lambda): PB: 2.7 caudal, 1.0 lateral, and 3.3 ventral; PAG: 1.9 caudal, 0.60 lateral, and 2.9 ventral. The skin was closed with Vetbond and the pups returned to the home cage for 1–3 d before the beginning of the electrophysiological experiments.

Retrograde labeling of spinal motor neurons with rhodamine dextran

Following the recording of lamina I pacemaker neurons (and intracellular dialysis with biocytin), the spinal cord was transferred to a circulating bath which was perfused with oxygenated aCSF at room temperature. Suction electrodes were fabricated from glass pipets (25 μl; Drummond Scientific Co., Broomall, PA) that were heated and pulled manually using forceps to produce a long taper. The glass was cut to produce a pore slightly larger in size than the L4 or L5 ventral root and fire-polished. The ventral root was drawn into a suction electrode under slight negative pressure, excess aCSF was removed from the electrode (via the back) with a plastic microcapillary, and the electrode was then filled with 1-2 μl of 1% tetramethylrhodamine dextran (Invitrogen). The spinal cord was perfused overnight with oxygenated aCSF to allow time for the dextran to retrogradely transport. The spinal cord was then fixed with 4% PFA (in 0.1 M PB), washed in PBS and embedded in gelatin overnight. Transverse sections (50 μm) were cut on a vibratome (Vibratome Company, St. Louis, MO), rinsed with PBS, and processed for biocytin staining as described above. Sections were then mounted on slides (Fisher Scientific, Florence, KY) with Vectashield mounting medium. Sections were examined through a 40X lens using an Olympus BX61 fluorescent microscope equipped with a spinning disc confocal unit, and scanned with a z-separation of 0.5 μm.

Pseudorabies virus (PRV) injections

Pseudorabies virus recombinant 152 (PRV-152; expressing GFP) was a kind gift from Dr. Lynn Enquist (Princeton University). The stock (at a titer of 2.89×10^8 pfu/ml) was stored at −80°C in 20 μl aliquots until just before use. A fresh aliquot of viral stock was thawed for each set of injections. At P1-P2, Sprague Dawley rat pups (n = 65) were anesthetized with isofluorane (3-4%). Small skin incisions were made to expose the left hindlimb quadriceps or left biceps femoris muscle. Two or three injections, together totaling 3 μl of viral stock, were made in the exposed muscle using a Hamilton 10 μl syringe equipped with a 33 gauge needle. Injection sites were blotted with a cotton swab to prevent the spread of excess virus to adjacent tissues and incisions were closed with 7-0 sutures (Ethicon; Cornelia, GA).

To examine the time course of PRV infection, at 24 - 72 hours post-infection (p.i.), animals were killed via sodium pentobarbital injection, perfused with 4% paraformaldehyde in PBS, and decapitated. Lumbar spinal cords were harvested and immersion-fixed an additional 4 hours in 4% paraformaldehyde in PBS. Tissue was then processed for GFP immunohistochemistry as described previously. To investigate the relationship between lamina I pacemakers and PRV-labeled spinal neurons, infected animals were killed 40 to 48 hours p.i. (via sodium pentobarbital injection) and prepared for patch clamp recording in the intact spinal cord. Following the intracellular dialysis of pacemaker neurons with biocytin,

the spinal cords were processed for biocytin visualization and immunohistochemistry as described above.

Imaging

Images were captured on a Zeiss LSM710 confocal microscope using either a 10X or 20X dry objective, or a 63X oil-immersion objective. For z-stack images, the interval between optical sections is 0.5 μm unless specified otherwise. The majority of image analysis was performed using LSM Image Browser (Zeiss). This included measurements of the cross-sectional area of pacemaker somata, in which the closed free shape curve tool was used to outline the cell body and the measure tool was then employed to calculate the area enclosed by the outline. To create composite images reconstructing the axonal morphology of biocytin-filled neurons, serial sections were photographed as described above. Individual images were pasted as sequential layers in Photoshop CS5 (Adobe), using fiducial points (including blood vessels and the central canal) to visually align images. Layers were then blended so that the complete labeled structure was visible.

Data analysis and statistics

Electrophysiological data were analyzed using Clampfit (Molecular Devices) software. Neurons were classified as bursting (i.e. pacemakers) if they exhibited clear plateau potentials which produce a distinct second peak on an all-points histogram of the membrane potential (Li and Baccei, 2011). Statistical differences between groups were determined using Student's t-tests, Mann-Whitney tests or Fisher's exact tests (Prism, GraphPad Software, La Jolla CA) as indicated in the text. $p < 0.05$ was considered significant. *n* refers to the number of neurons sampled in a given group unless stated otherwise. Data are expressed as means ± SEM.

Results

Identification of pacemaker neurons in the intact spinal cord

Whole-cell patch clamp recordings were obtained from neonatal (P1-P5) lamina I neurons using an *in vitro* intact spinal cord preparation (Safronov et al., 2007; Szucs et al., 2009). A subpopulation of sampled neurons (65 of 162; 40%) exhibited rhythmic burst-firing (Fig. 1A) that defines pacemaker activity in the SDH. As reported previously (Li and Baccei, 2011; Li et al., 2013), most pacemakers in lamina I were judged to be relatively small in size based on measurements of their membrane capacitance (<50 pF). Since our prior work demonstrated that fusiform, multipolar and pyramidal subtypes of lamina I neurons are all capable of generating pacemaker activity (Li and Baccei, 2011), dendritic morphology was not the focus of the present study. Interestingly, the current results suggest that lamina I pacemaker neurons exhibit three distinct patterns in terms of their axonal projections. In one group (n = 12), a main axon could be observed to course medially and ventrally through the superficial dorsal horn (SDH) and deep dorsal horn (DDH) before proceeding to the lateral edge of the intermediate gray matter where it gave rise to numerous collateral branches (Fig. 1B). Meanwhile, other pacemakers had axons which curved around the lateral edge of the dorsal gray matter and coursed towards the anterior commissure (Fig. 1C), or which ramified solely within the SDH (Fig. 1D). Of the 27 small pacemakers examined, 12

projected to the DDH (Fig. 1B), 6 had axons that reached or crossed the anterior commissure, and 9 possessed axons that were restricted to the superficial laminae.

Immunohistochemical analysis demonstrated that, in 6 of 7 pacemakers examined, the axonal boutons in the deep dorsal horn expressed the vesicular glutamate transporter VGLUT2 (Fig. 1E-G), indicating the glutamatergic phenotype of the pacemaker neurons. This is consistent with our previous findings (7 of 8 pacemakers shown to express VGLUT2) using spinal cord slices (Li and Baccei, 2011). Importantly, these results demonstrate that lamina I pacemakers send excitatory projections ventrally in the spinal cord during early postnatal development.

Putative contacts between lamina I pacemakers and motor neurons in the neonatal spinal cord

Since a fraction (5 of 14) of lamina I pacemakers were previously found to project into the spinal ventral horn (Li and Baccei, 2011), we next investigated the possibility that motor neurons were contacted by the axons of pacemaker neurons. In order to effectively visualize the somata and dendrites of motor neurons, following the patch clamp recordings from pacemakers in lamina I (n = 6 rats), motor neurons were retrogradely labeled via the application of rhodamine dextran to the L4 or L5 ventral root (Fig. 2A). This approach produced robust labeling of the motor neuron dendrites (Fig. 2B) which were often seen to extend dorsally into the deep dorsal horn, as has been reported previously (Kalb, 1994). More importantly, putative contacts between the pacemaker axons and the motor neuron dendrites could be seen (Fig. 2C).

Retrograde tracing of spinal motor pathways using pseudorabies virus (PRV)

Pacemakers in the SDH could also strongly modulate the motor output of the neonatal spinal cord via their interactions with premotor interneurons which are densely populated within the deep dorsal horn (Jovanovic et al., 2010; Tripodi et al., 2011). To examine this hypothesis, we back-labeled the neuronal pathway originating from flexor (biceps femoris) and extensor (quadriceps) muscles of the left hindlimb using the GFP-expressing pseudorabies virus PRV-152, a recombinant PRV-Bartha strain that is known to be retrogradely transported across synapses (Smith et al., 2000). Prior studies have shown that intramuscular PRV-152 injection in rodents leads to the infection of motor neurons innervating the injected muscle, followed by retrograde transport of the virus to premotor interneurons in the spinal cord (Jovanovic et al., 2010).

To characterize the time course of PRV spread in neonatal rats, PRV-152 was injected into the biceps femoris or quadriceps at P1-P2 (n = 14 rats) and GFP expression in the spinal cord was monitored at 4 hour intervals from 24 - 60 hours post-infection (p.i.). Labeled motor neurons were detected as early as 24 hour p.i. (Fig. 3A), with GFP-labeled premotor interneurons evident in the ventral and deep dorsal horn between 32 - 44 hours p.i. (Fig. 3B-C). Notably, superficial dorsal horn (SDH) neurons were clearly infected by 48 - 52 hours p.i., while sparse GFP expression was observed within presumptive lamina III-IV at this time point (Fig. 3D). Overall, this time course is highly consistent with that previously

reported in the neonatal mouse (Jovanovic et al., 2010), although PRV-152 labeling within the SDH was not specifically commented upon in that study.

GFP expression in the sensorimotor cortex was detected at 72 hours p.i (*data not shown*). Importantly, no GFP labeling was detected anywhere in the brain prior to 66 hours p.i., excluding the possibility that viral infection had reached the brain and was transported back to the spinal cord at the 24 - 52 hour time points (Fig. 3). In addition, evidence shows that PRV-152 is not transported to dorsal horn neurons via primary afferents innervating the muscle (Jovanovic et al., 2010), which agrees with earlier observations that the distribution of labeled lamina I-II neurons after injection of PRVBartha into the muscle was not significantly altered by dorsal rhizotomy (Jasmin et al., 1997). Therefore, the infection of SDH neurons can be attributed to retrograde transport along spinal motor pathways rather than via sensory pathways entering the spinal cord via the dorsal root.

Pacemakers innervate premotor interneurons that synapse onto flexor motor neurons

Based on the time course of PRV-152 labeling in the spinal cord (Fig. 3), we chose a window of 40 - 46 hours post-infection (p.i.) to investigate the connectivity between lamina I pacemakers and premotor interneurons located ipsilaterally to the virus injection into the biceps femoris (n = 11 rats). Pacemaker axons filled with biocytin exhibited varicosities which were in close apposition to both cell bodies and dendrites of PRV-infected interneurons in the ipsilateral deep dorsal horn (Fig. 4A) and ventral horn (Fig. 4B, C) of the neonatal spinal cord. Fig. 4D illustrates an example of pacemaker axonal boutons showing VGLUT1/2 immunoreactivity in close apposition to a PRV-152 infected cell in the deep dorsal horn, suggesting that at least some of the axonal varicosities located in proximity to PRV-infected cells represent synapses.

If the above appositions do correspond to synaptic contacts between the pacemakers and premotor interneurons, one would predict that the lamina I pacemakers would eventually become infected with PRV-152 themselves with longer post-infection survival times (see Fig. 3D). Therefore, to provide further support for the notion that lamina I pacemaker neurons connect to spinal motor pathways during early life, we obtained patch clamp recordings from PRV-infected (i.e. GFP-expressing) lamina I neurons at 48 - 54 hours following PRV injections into the biceps femoris. Critically, PRV-infected lamina I neurons were observed to exhibit the rhythmic burst-firing that defines pacemaker activity in the SDH, as evidenced by the co-localization of biocytin labeling with GFP immunoreactivity (Fig. 4E-H). Given that PRV-152 is retrogradely transported across synapses, these results strongly argue that lamina I pacemaker neurons are synaptically coupled to the motor pathways innervating the biceps femoris muscle of the hindlimb.

Lamina I pacemakers engage extensor motor pathways in the lumbar spinal cord

We next investigated whether pacemakers in the neonatal SDH selectively contact motor pathways innervating flexor or extensor muscles in the hindlimb. A similar experimental approach was used as described above, except the PRV-152 was injected into the left quadriceps muscles to label extensor motor pathways (n = 9 rats). At 40 - 46 hours post-infection (p.i.), the axonal boutons of functionally identified pacemakers were observed in

close apposition to the somata and dendrites of PRV-152 infected cells in the ipsilateral deep dorsal horn (Fig. 5A-D) and ventral horn (Fig. 5E-F). Meanwhile, at 48 - 54 hours p.i., we documented the presence of rhythmically-bursting lamina I neurons that clearly expressed GFP (Fig. 5G-J), indicating that the PRV-152 was retrogradely transported to infect the pacemaker population at this time point. These results suggest that pacemakers form synapses onto the spinal interneurons which lie upstream of the motor neurons innervating the quadriceps muscles.

Interestingly, we observed no evidence of a preferential innervation of flexor or extensor motor circuits by pacemaker neurons in the developing spinal cord. Of the 14 pacemakers examined in conjunction with retrograde labeling of the flexor pathway, 8 (~57%) were observed to contact premotor interneurons infected with PRV-152. Meanwhile, 9 of 16 (~56%) pacemakers projected axons in close proximity to interneurons retrogradely labeled via PRV injection into the extensor muscles. In addition, pacemakers appeared to make a similar number of putative axonal contacts (per cell) onto premotor interneurons in the flexor (3.86 ± 0.95 contacts; n = 8 pacemakers) and extensor (2.88 ± 0.66 contacts; n = 9; p = 0.299; Mann-Whitney test) motor pathways. To characterize the cellular distribution of pacemaker axonal contacts onto their putative postsynaptic targets, we calculated the percentage of pacemaker boutons which lay in apposition to the somata vs. dendrites of the PRV-infected interneurons (data pooled from the flexor and extensor pathways). Approximately 46% (26 of 56) of the boutons examined were located in proximity to the cell bodies of the premotor interneurons, while 54% (30 of 56) of the putative contacts were observed in apposition to the dendrites of these cells.

Ascending lamina I projection neurons as pacemakers in the neonatal spinal cord

While the majority of pacemaker neurons recorded using the intact spinal cord preparation exhibited a membrane capacitance (C_m) of less than 50 pF, we did observe rhythmic burst-firing in a population of larger lamina I neurons that was not evident in the spinal cord slice (Fig. 6A, *arrow*; see also Li and Baccei, 2011). In instances where an intact cell body was recovered and clearly visible, both C_m and cross-sectional area were used to classify cell size, otherwise C_m alone was used. Pacemakers with a C_m of greater than 50 pF and a cross-sectional area of more than 160 μm^2 were classified as large for the purposes of the present study. This classification method revealed two distinct groups as measured by C_m (Large: Mean C_m = 72.5 ± 4.9 pF; range: 52-102 pF; n = 14; Small: Mean C_m = 34.4 ± 1.9 pF; range: 20-50 pF; n = 17; $p < 0.0001$; unpaired t-test) and area (Large: 242.3 ± 13.1 μm^2; Small: 133.6 ± 9.4 μm^2; $p < 0.0001$).

Interestingly, the axonal projection patterns of these larger pacemakers displayed striking differences compared to those of the smaller pacemaker neurons. First, the axons of large pacemakers did not exhibit branching off the main axon in the deep dorsal horn (Fig. 6B), in contrast to the extensive branching seen with the smaller pacemaker neurons (Fig. 1B). In 23 of the 29 large pacemakers examined, the axons coursed laterally along the dorsal edge of the gray matter and appeared to follow the curvature of the lateral edge of the dorsal horn before crossing medially through the deep dorsal horn and ventral horn (Fig. 6B). The axons were often observed to enter the anterior commissure and in many cases the fibers could be

seen in the ventral white matter on the contralateral side (see *arrow* in Fig. 6B). Fig. 6C illustrates an example of a parasagittal spinal cord section taken from the side contralateral to the pacemaker soma, showing a biocytin-filled axon that projects rostrally in the white matter after crossing the midline. These rostral projections could be followed for <1 mm, which may reflect limitations in the axonal transport of the biocytin from the soma of the lamina I neuron during the recording period. Consistent with the presence of two subpopulations of pacemakers in lamina I, rhythmically bursting neurons with axons that crossed to the contralateral side of the spinal cord possessed significantly higher C_m compared to pacemakers whose axons remained ipsilaterally (Contralateral: 65.0 ± 4.4 pF, n = 23; Ipsilateral: 34.8 ± 2.0 pF, n = 17; $p < 0.0001$, Student's t-test).

It is important to note that both small and large pacemakers established putative axonal contacts with PRV-152 labeled neurons comprising the flexor and extensor motor pathways, although the majority (14 of 17) of these pacemakers were classified as small. While the mean number of putative contacts onto PRV-labeled interneurons (per pacemaker) appeared similar between the small (3.50 ± 0.67 contacts, n = 14) and large (2.33 ± 0.33 contacts; n = 3) pacemakers examined, it should be noted that the limited number of rhythmically bursting neurons that were confirmed to express GFP at the 48 - 54 hour post-infection time point (Fig. 4E-H, 5G-J) were all classified as small (n = 4).

Based on patch clamp recordings in the spinal cord slice preparation, we have previously reported that identified spino-parabrachial (spino-PB) and spino-PAG projection neurons in lamina I fail to exhibit rhythmic burst-firing during the first week of life (Li and Baccei, 2011; Li and Baccei, 2012). However, the axonal morphology of the large lamina I pacemakers in the present study (Fig. 6) was strikingly similar to the previously described trajectory of axons belonging to lamina I projection neurons (Szucs et al., 2010). Given the better preservation of cellular integrity with the intact spinal cord preparation and the clear dependence of pacemaker activity on the presence of high membrane resistance (Li and Baccei, 2011; Li et al., 2013), it is possible that damage incurred during the slicing procedure resulted in a loss of rhythmic burst-firing within the projection neurons sampled in our prior slice recordings. Therefore, we revisited this issue in the present study using patch clamp recordings from identified spino-parabrachial and spino-PAG projection neurons within the intact spinal cord (Fig. 7A, B).

The results clearly demonstrate that both spino-PB and spino-PAG lamina I projection neurons can exhibit rhythmic burst-firing during early postnatal development (Fig. 7C, D). This spontaneous activity generally involved slow plateau-like depolarizations (often >1 sec in duration) with bursts of action potential discharge superimposed upon these oscillations (Fig. 7C), as we reported previously (Li and Baccei, 2011; Li et al., 2013). However, a minority of bursting projection neurons exhibited rhythmic depolarizations of shorter duration which were often accompanied by spike doublets (Fig. 7D). The average C_m measured in the spino-PB and spino-PAG neurons that exhibited rhythmic burst-firing (91.0 ± 7.0 pF, n = 9) is consistent with the notion that these cells correspond to the large pacemakers within the intact SDH that are not observed in spinal cord slices. Notably, there was no significant difference in the prevalence of pacemaker activity between the spino-PB

(4 of 41 neurons sampled) and spino-PAG (5 of 37) populations during the neonatal period ($p = 0.729$; Fisher's exact test; Fig. 7E).

Discussion

The present study is the first to investigate the connectivity of pacemaker neurons located within lamina I of the neonatal superficial dorsal horn (SDH). Our data demonstrate that at least one population of rhythmically bursting neurons engages both flexor and extensor motor pathways in the developing spinal cord (Fig. 8). In addition, pacemakers also directly target brain regions known to be critically involved in nociceptive processing, as a fraction of pacemakers were conclusively identified as ascending spino-parabrachial and spino-PAG projection neurons. Collectively, the results suggest that pacemakers in the SDH are positioned to modulate both the motor output of the spinal cord network and neuronal activity within supraspinal nociceptive circuits. Therefore, lamina I pacemakers may contribute to the activity-dependent maturation of central pain and sensorimotor networks during early postnatal development.

Lamina I pacemakers engage motor networks in the developing spinal cord

Spontaneous activity is a prominent feature of spinal motor neurons during the embryonic period (O'Donovan et al., 1994; Nakayama et al., 1999; Busetto et al., 2003; Ren and Greer, 2003) and is thought to be essential for the normal maturation of the motor network, via its effects on a range of processes including axonal pathfinding (Kastanenka and Landmesser, 2010; Kastanenka and Landmesser, 2013), regulation of synapse number in muscle fibers (Thompson, 1983; Ribchester and Taxt, 1983) and normal muscle development (Roufa and Martonosi, 1981). The available evidence suggests that this spontaneous firing at least partly originates within the spinal cord itself, as the activity persists following spinal transection or deafferentation (Blumberg and Lucas, 1994; Robinson et al., 2000; Waldenstrom et al., 2009). Candidate mechanisms include an enhanced intrinsic membrane excitability of immature motor neurons (Viana et al., 1994; Seebach and Mendell, 1996), electrotonic coupling via gap junctions (Walton and Navarrete, 1991), and/or synaptic excitation from a network of premotor interneurons (Milner and Landmesser, 1999; Wenner and O'Donovan, 2001; Hanson and Landmesser, 2003). Interestingly, at early stages of development, bursts of activity in spinal interneurons are well-correlated with the generation of spontaneous muscle contractions (Rosato-Siri et al., 2004).

The present results demonstrate that small lamina I pacemaker neurons contact premotor interneurons in the neonatal spinal cord, which could facilitate spontaneous activity within both flexor and extensor motor neurons during early life. We have confirmed that the varicosities of pacemaker axons located in the deeper regions of the spinal cord express the vesicular glutamate transporter VGLUT2 (Fig. 1; see Li and Baccei 2011). Nonetheless, it should be noted that the close apposition of pacemaker boutons and PRV-infected interneurons (Fig. 4, 5), or motor neurons identified with rhodamine dextran transport (Fig. 2), does not guarantee the presence of functional synapses between these cell types. Indeed, since recent studies suggest that only ~20% of observed axodendritic contacts actually

correspond to synapses (Mishchenko et al., 2010), ultra-structural analysis would be necessary to unambiguously confirm that these close appositions reflect synapses.

However, given the wealth of evidence showing that the modified PRV-Bartha strains are transported across synapses in the CNS (Card et al., 1993; Rinaman et al., 1999; Pickard et al., 2002), along with our observations that small PRV-infected lamina I neurons can themselves exhibit rhythmic burst-firing during the neonatal period (Fig. 4E-H, 5G-J), it appears highly probable that at least a fraction of the observed appositions reflect functional synaptic connections between small lamina I pacemakers and the flexor and extensor motor pathways in the developing spinal cord. While the number of documented contacts between a single pacemaker and the population of premotor interneurons was low, our measurements represent an underestimation, as focal injection of PRV into a given muscle does not label the entire group of relevant premotor interneurons. In addition, while we examined the connectivity of individual pacemakers, a given premotor interneuron likely receives input from multiple pacemakers that may summate to drive postsynaptic action potential discharge. Nonetheless, further experiments are needed to confirm that pacemaker connections are strong enough to evoke motor activity during early life. It should also be noted that the extent to which large pacemakers engage spinal motor pathways remains to be fully elucidated, as most putative synaptic contacts onto premotor interneurons were associated with small pacemakers, and we have yet to confirm that large PRV-infected lamina I neurons can also exhibit rhythmic burst-firing.

One caveat to consider is that while evidence strongly suggests the PRV is not transported to the spinal cord via primary afferents, PRV injected into hindlimb muscles can strongly infect sympathetic efferents (Rotto-Percelay et al., 1992). Therefore, while our recordings were obtained in the lumbar enlargement, at a distance from the interomediolateral (IML) cell column at T11-L2, we cannot completely exclude the possibility that L4-L5 lamina I neurons could become labeled with PRV via retrograde transport along sympathetic pathways (and connections between lumbar dorsal horn cells and the IML) rather than via synapses onto motor circuits in the ventral horn. The question of whether lamina I pacemakers synapse directly onto spinal motor neurons also warrants further investigation. While the close appositions of pacemaker axons with motor neuron dendrites (Fig. 2) is consistent with the existence of direct connections between these populations, the PRV experiments show that lamina I neurons become infected at later time points compared to premotor interneurons in the deep dorsal horn (Fig. 3). This raises the possibility that the PRV must be transported through an intervening neuron in a polysynaptic pathway before reaching lamina I. This issue could be addressed with strategies involving the use of modified tracing viruses that can cross only one synapse in the retrograde direction (Wickersham et al., 2007).

It will also clearly be necessary to further characterize the populations of spinal interneurons which are innervated by lamina I pacemakers during early life, as the neurotransmitter phenotype of these interneurons will have functional implications for how pacemaker activity might shape the motor output to various muscle groups in the neonate. Therefore, further experiments will elucidate whether pacemaker axons contact glutamatergic, cholinergic or GABAergic/glycinergic cells in the deep dorsal horn and ventral horn, and

determine whether this connectivity differs between the flexor and extensor motor pathways. However, it should be noted that the activation of $GABA_A$ and glycine receptors in the embryonic spinal cord provides excitatory drive to the motor networks (Chub and O'Donovan, 1998; Wenner, 2014). While we have yet to examine the prevalence of pacemaker activity during the embryonic period, the high incidence of rhythmic burst-firing in lamina I during the first days of life makes it highly likely that some neurons exhibit pacemaker activity prior to birth. If so, SDH pacemakers could facilitate the excitation of developing spinal motor neurons via interneurons that are either glutamatergic or GABAergic/glycinergic in nature.

Pacemakers as putative drivers of activity within central nociceptive networks

There are multiple mechanisms by which the rhythmic burst-firing of lamina I neurons could regulate the level of excitability in nociceptive circuits of the CNS. First, the axons of pacemakers can ramify extensively within the SDH (Li and Baccei, 2011). Second, our present data indicate that a subpopulation of large pacemakers directly correspond to ascending projection neurons targeting the parabrachial nucleus (PB) and periaqueductal gray (PAG), which represent key supraspinal sites of nociceptive processing (Spike et al., 2003; Al-Khater and Todd, 2009). It remains to be determined if intrinsic bust-firing selectively occurs in neonatal projection neurons within the SDH or whether projection neurons in deeper laminae also exhibit pacemaker activity, as adult deep dorsal horn neurons are capable of endogenous burst-firing subject to tight metabotropic control (Derjean et al., 2003). Notably, while we rarely observed axon collaterals in the sampled population of large pacemakers, prior studies (using a fivefold higher concentration of intracellular biocytin) have clearly shown that lamina I projection neurons innervate other lamina I neurons (including other projection neurons) in addition to their targets in the brain (Szucs et al., 2010). This raises the possibility that pacemaker activity in ascending projection neurons provides an endogenous excitatory drive to both supraspinal nociceptive networks as well as the local SDH circuit during the early postnatal period.

Pacemakers in lamina I could also modulate neuronal activity within the SDH indirectly, via their projections to spinal motor networks. Spontaneous muscle activity creates skin movement that provides innocuous mechanosensory feedback to the immature SDH, possibly via the ectopic Aβ primary afferents that innervate lamina I-II during early life (Fitzgerald et al., 1994; Beggs et al., 2002), which is necessary for the normal development of the nociceptive withdrawal reflex (NWR) (Petersson et al., 2003; Waldenstrom et al., 2003). A theoretical framework to explain this cross-modal maturation of the NWR proposes the existence of "reflex encoders" in the spinal cord which generate spontaneous burst-firing and thus facilitate the activation of motor neurons in the ventral horn (Schouenborg, 2008). We speculate that small lamina I pacemakers could serve as reflex encoders during the early postnatal period, via their ventrally-oriented projections to premotor interneurons in the deep dorsal and ventral horn of the spinal cord. Although the pacemakers did not preferentially innervate flexor motor pathways, an appropriate NWR does require the coordination of ipsilateral flexion and contralateral extension. This could explain why pacemakers are positioned to provide intrinsic excitatory drive to both flexor and extensor motor circuits during early life. Unfortunately, the present study is unable to

reveal the eventual fate of the pacemaker projections to pre-motor interneurons. If these connections do persist beyond the developmental decline in spontaneous burst-firing within the SDH (Li and Baccei, 2011), they may contribute to the generation of withdrawal reflexes in response to noxious sensory input during adulthood.

While further studies are clearly essential, collectively the present evidence suggests that the function of lamina I pacemaker neurons is not restricted to the local processing of nociceptive signals within the newborn superficial dorsal horn, and may instead extend to sensorimotor integration in the developing spinal cord as well as a potential facilitatory role in the activity-dependent maturation of pain networks in the brain.

Acknowledgements

This work was supported by the National Institutes of Health (NS072202 to MLB).

The authors would like to thank Dr. Lynn Enquist for kindly providing the PRV-152 and Drs. Fumiyasu Imai, Masaki Ueno, Yutaka Yoshida and Michael O'Donovan for technical advice on this project. We also thank Dr. Yutaka Yoshida for helpful feedback regarding the manuscript.

Literature Cited

Al-Khater KM, Todd AJ. Collateral projections of neurons in laminae I, III, and IV of rat spinal cord to thalamus, periaqueductal gray matter, and lateral parabrachial area. J Comp Neurol. 2009; 515:629–46. [PubMed: 19496168]

Beggs S, Torsney C, Drew LJ, Fitzgerald M. The postnatal reorganization of primary afferent input and dorsal horn cell receptive fields in the rat spinal cord is an activity-dependent process. Eur J Neurosci. 2002; 16:1249–58. [PubMed: 12405985]

Blumberg MS, Lucas DE. Dual mechanisms of twitching during sleep in neonatal rats. Behav Neurosci. 1994; 108:1196–202. [PubMed: 7893412]

Busetto G, Buffelli M, Cangiano L, Cangiano A. Effects of evoked and spontaneous motoneuronal firing on synapse competition and elimination in skeletal muscle. J Neurocytol. 2003; 32:795–802. [PubMed: 15034268]

Card JP, Rinaman L, Lynn RB, Lee BH, Meade RP, Miselis RR, Enquist LW. Pseudorabies virus infection of the rat central nervous system: ultrastructural characterization of viral replication, transport, and pathogenesis. J Neurosci. 1993; 13:2515–39. [PubMed: 8388923]

Chub N, O'Donovan MJ. Blockade and recovery of spontaneous rhythmic activity after application of neurotransmitter antagonists to spinal networks of the chick embryo. J Neurosci. 1998; 18:294–306. [PubMed: 9412508]

Derjean D, Bertrand S, Le Masson G, Landry M, Morisset V, Nagy F. Dynamic balance of metabotropic inputs causes dorsal horn neurons to switch functional states. Nat Neurosci. 2003; 6:274–81. [PubMed: 12592405]

Fitzgerald M, Butcher T, Shortland P. Developmental changes in the laminar termination of A fibre cutaneous sensory afferents in the rat spinal cord dorsal horn. J Comp Neurol. 1994; 348:225–33. [PubMed: 7814689]

Hanson MG, Landmesser LT. Characterization of the circuits that generate spontaneous episodes of activity in the early embryonic mouse spinal cord. J Neurosci. 2003; 23:587–600. [PubMed: 12533619]

Hoorneman EM. Stereotaxic operation in the neonatal rat; a novel and simple procedure. J Neurosci Methods. 1985; 14:109–16. [PubMed: 2993760]

Jovanovic K, Pastor AM, O'Donovan MJ. The use of PRV-Bartha to define premotor inputs to lumbar motoneurons in the neonatal spinal cord of the mouse. PLoS One. 2010; 5:e11743. [PubMed: 20668534]

Kalb RG. Regulation of motor neuron dendrite growth by NMDA receptor activation. Development. 1994; 120:3063–71. [PubMed: 7720552]

Kastanenka KV, Landmesser LT. In vivo activation of channelrhodopsin-2 reveals that normal patterns of spontaneous activity are required for motoneuron guidance and maintenance of guidance molecules. J Neurosci. 2010; 30:10575–85. [PubMed: 20686000]

Kastanenka KV, Landmesser LT. Optogenetic-mediated increases in in vivo spontaneous activity disrupt pool-specific but not dorsal-ventral motoneuron pathfinding. Proc Natl Acad Sci U S A. 2013; 110:17528–33. [PubMed: 24101487]

Landry M, Bouali-Benazzouz R, El Mestikawy S, Ravassard P, Nagy F. Expression of vesicular glutamate transporters in rat lumbar spinal cord, with a note on dorsal root ganglia. J Comp Neurol. 2004; 468:380–94. [PubMed: 14681932]

Li J, Baccei ML. Pacemaker neurons within newborn spinal pain circuits. J Neurosci. 2011; 31:9010–22. [PubMed: 21677184]

Li J, Baccei ML. Developmental regulation of membrane excitability in rat spinal lamina I projection neurons. J Neurophysiol. 2012; 107:2604–14. [PubMed: 22338021]

Li J, Blankenship ML, Baccei ML. Inward-rectifying potassium (Kir) channels regulate pacemaker activity in spinal nociceptive circuits during early life. J Neurosci. 2013; 33:3352–62. [PubMed: 23426663]

Lischalk JW, Easton CR, Moody WJ. Bilaterally propagating waves of spontaneous activity arising from discrete pacemakers in the neonatal mouse cerebral cortex. Dev Neurobiol. 2009; 69:407–14. [PubMed: 19263415]

Milner LD, Landmesser LT. Cholinergic and GABAergic inputs drive patterned spontaneous motoneuron activity before target contact. J Neurosci. 1999; 19:3007–22. [PubMed: 10191318]

Mishchenko Y, Hu T, Spacek J, Mendenhall J, Harris KM, Chklovskii DB. Ultrastructural analysis of hippocampal neuropil from the connectomics perspective. Neuron. 2010; 67:1009–20. [PubMed: 20869597]

Nakayama K, Nishimaru H, Iizuka M, Ozaki S, Kudo N. Rostrocaudal progression in the development of periodic spontaneous activity in fetal rat spinal motor circuits in vitro. J Neurophysiol. 1999; 81:2592–5. [PubMed: 10322093]

O'Donovan M, Ho S, Yee W. Calcium imaging of rhythmic network activity in the developing spinal cord of the chick embryo. J Neurosci. 1994; 14:6354–69. [PubMed: 7965041]

Petersson P, Waldenstrom A, Fahraeus C, Schouenborg J. Spontaneous muscle twitches during sleep guide spinal self-organization. Nature. 2003; 424:72–5. [PubMed: 12840761]

Pickard GE, Smeraski CA, Tomlinson CC, Banfield BW, Kaufman J, Wilcox CL, Enquist LW, Sollars PJ. Intravitreal injection of the attenuated pseudorabies virus PRV Bartha results in infection of the hamster suprachiasmatic nucleus only by retrograde transsynaptic transport via autonomic circuits. J Neurosci. 2002; 22:2701–10. [PubMed: 11923435]

Ren J, Greer JJ. Ontogeny of rhythmic motor patterns generated in the embryonic rat spinal cord. J Neurophysiol. 2003; 89:1187–95. [PubMed: 12626606]

Ribchester RR, Taxt T. Motor unit size and synaptic competition in rat lumbrical muscles reinnervated by active and inactive motor axons. J Physiol. 1983; 344:89–111. [PubMed: 6655594]

Rinaman L, Roesch MR, Card JP. Retrograde transynaptic pseudorabies virus infection of central autonomic circuits in neonatal rats. Brain Res Dev Brain Res. 1999; 114:207–16.

Robinson SR, Blumberg MS, Lane MS, Kreber LA. Spontaneous motor activity in fetal and infant rats is organized into discrete multilimb bouts. Behav Neurosci. 2000; 114:328–36. [PubMed: 10832794]

Rosato-Siri MD, Zoccolan D, Furlan F, Ballerini L. Interneurone bursts are spontaneously associated with muscle contractions only during early phases of mouse spinal network development: a study in organotypic cultures. Eur J Neurosci. 2004; 20:2697–710. [PubMed: 15548213]

Rotto-Percelay DM, Wheeler JG, Osorio FA, Platt KB, Loewy AD. Transneuronal labeling of spinal interneurons and sympathetic preganglionic neurons after pseudorabies virus injections in the rat medial gastrocnemius muscle. Brain Res. 1992; 574:291–306. [PubMed: 1322222]

Roufa D, Martonosi AN. Effect of curare on the development of chicken embryo skeletal muscle in ovo. Biochem Pharmacol. 1981; 30:1501–5. [PubMed: 6456003]

Safronov BV, Pinto V, Derkach VA. High-resolution single-cell imaging for functional studies in the whole brain and spinal cord and thick tissue blocks using light-emitting diode illumination. J Neurosci Methods. 2007; 164:292–8. [PubMed: 17586052]

Schouenborg J. Action-based sensory encoding in spinal sensorimotor circuits. Brain Res Rev. 2008; 57:111–7. [PubMed: 17920132]

Seebach BS, Mendell LM. Maturation in properties of motoneurons and their segmental input in the neonatal rat. J Neurophysiol. 1996; 76:3875–85. [PubMed: 8985885]

Sipila ST, Huttu K, Soltesz I, Voipio J, Kaila K. Depolarizing GABA acts on intrinsically bursting pyramidal neurons to drive giant depolarizing potentials in the immature hippocampus. J Neurosci. 2005; 25:5280–9. [PubMed: 15930375]

Smith BN, Banfield BW, Smeraski CA, Wilcox CL, Dudek FE, Enquist LW, Pickard GE. Pseudorabies virus expressing enhanced green fluorescent protein: A tool for in vitro electrophysiological analysis of transsynaptically labeled neurons in identified central nervous system circuits. Proc Natl Acad Sci U S A. 2000; 97:9264–9. [PubMed: 10922076]

Spike RC, Puskar Z, Andrew D, Todd AJ. A quantitative and morphological study of projection neurons in lamina I of the rat lumbar spinal cord. Eur J Neurosci. 2003; 18:2433–48. [PubMed: 14622144]

Szucs P, Luz LL, Lima D, Safronov BV. Local axon collaterals of lamina I projection neurons in the spinal cord of young rats. J Comp Neurol. 2010; 518:2645–65. [PubMed: 20506469]

Szucs P, Pinto V, Safronov BV. Advanced technique of infrared LED imaging of unstained cells and intracellular structures in isolated spinal cord, brainstem, ganglia and cerebellum. J Neurosci Methods. 2009; 177:369–80. [PubMed: 19014968]

Tazerart S, Viemari JC, Darbon P, Vinay L, Brocard F. Contribution of persistent sodium current to locomotor pattern generation in neonatal rats. J Neurophysiol. 2007; 98:613–28. [PubMed: 17567773]

Tazerart S, Vinay L, Brocard F. The persistent sodium current generates pacemaker activities in the central pattern generator for locomotion and regulates the locomotor rhythm. J Neurosci. 2008; 28:8577–89. [PubMed: 18716217]

Thompson W. Synapse elimination in neonatal rat muscle is sensitive to pattern of muscle use. Nature. 1983; 302:614–6. [PubMed: 6835395]

Todd AJ. Neuronal circuitry for pain processing in the dorsal horn. Nat Rev Neurosci. 2010; 11:823–36. [PubMed: 21068766]

Tripodi M, Stepien AE, Arber S. Motor antagonism exposed by spatial segregation and timing of neurogenesis. Nature. 2011; 479:61–6. [PubMed: 22012263]

Tritsch NX, Rodriguez-Contreras A, Crins TT, Wang HC, Borst JG, Bergles DE. Calcium action potentials in hair cells pattern auditory neuron activity before hearing onset. Nat Neurosci. 2010; 13:1050–2. [PubMed: 20676105]

Viana F, Bayliss DA, Berger AJ. Postnatal changes in rat hypoglossal motoneuron membrane properties. Neuroscience. 1994; 59:131–48. [PubMed: 8190264]

Waldenstrom A, Christensson M, Schouenborg J. Spontaneous movements: Effect of denervation and relation to the adaptation of nociceptive withdrawal reflexes in the rat. Physiol Behav. 2009; 98:532–6. [PubMed: 19715712]

Waldenstrom A, Thelin J, Thimansson E, Levinsson A, Schouenborg J. Developmental learning in a pain-related system: evidence for a cross-modality mechanism. J Neurosci. 2003; 23:7719–25. [PubMed: 12930812]

Walton KD, Navarrete R. Postnatal changes in motoneurone electrotonic coupling studied in the in vitro rat lumbar spinal cord. J Physiol. 1991; 433:283–305. [PubMed: 1668753]

Wenner P. Homeostatic synaptic plasticity in developing spinal networks driven by excitatory GABAergic currents. Neuropharmacology. 2014; 78:55–62. [PubMed: 23727439]

Wenner P, O'Donovan MJ. Mechanisms that initiate spontaneous network activity in the developing chick spinal cord. J Neurophysiol. 2001; 86:1481–98. [PubMed: 11535692]

Wickersham IR, Lyon DC, Barnard RJ, Mori T, Finke S, Conzelmann KK, Young JA, Callaway EM. Monosynaptic restriction of transsynaptic tracing from single, genetically targeted neurons. Neuron. 2007; 53:639–47. [PubMed: 17329205]

Zheng J, Lee S, Zhou ZJ. A transient network of intrinsically bursting starburst cells underlies the generation of retinal waves. Nat Neurosci. 2006; 9:363–71. [PubMed: 16462736]

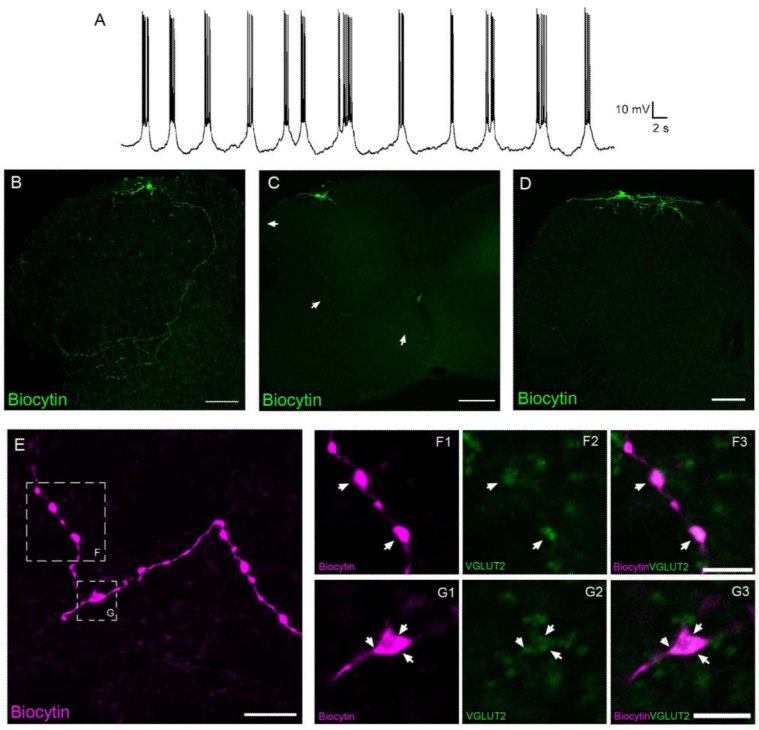

Figure 1.

Lamina I pacemakers send glutamatergic projections to multiple regions of the intact neonatal rat spinal cord. ***A,*** Example of the rhythmic burst-firing that characterizes pacemaker activity in the immature superficial dorsal horn (SDH). ***B, C, D,*** Composite images constructed from 11 ***(B)***, 5 ***(C)*** or 8 ***(D)*** overlaid serial sections (each 20 μm thick). While some pacemaker axons display extensive branching in the deep dorsal horn before reaching the lateral edge of the gray matter ***(B***; scale bar = 100 μm*)*, other pacemakers send relatively unbranched axons around the lateral edge of the dorsal horn and across the anterior commissure ***(C***; scale bar = 200 μm*)*. A third group of pacemakers was characterized by axons which ramified exclusively within the superficial laminae of the dorsal horn ***(D***; scale bar = 100 μm*)*. ***E,*** Image (consisting of a z-stack of 11 optical sections at a thickness of 0.5 μm) depicting a pacemaker axon located in the deep dorsal horn with several prominent boutons (*see boxed regions*). Scale bar = 10 μm. ***F, G,*** Single optical sections (0.5 μm) showing a higher magnification of the boxed regions indicated in panel ***E***, demonstrating that the axonal boutons of small pacemaker neurons (*magenta*) co-localize (*arrows*) with VGLUT2 immunoreactivity (*green*). Scale bars = 5 μm.

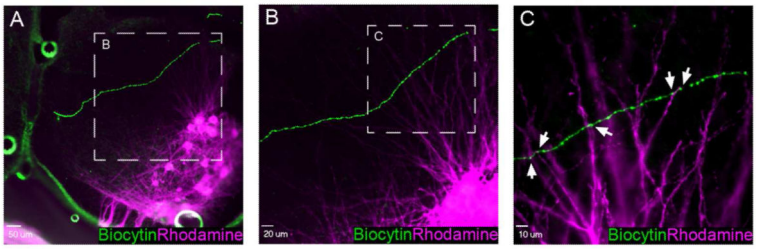

Figure 2.

Putative axodendritic contacts between pacemaker neurons and spinal motor neurons. ***A,*** Low magnification image showing a biocytin-filled axon (*green*) of an identified lamina I pacemaker neuron that travels through the deep dorsal horn of the spinal cord in a ventromedial direction. A pool of lumbar motor neurons (*magenta*) has been retrogradely labeled via rhodamine dextran applied to the L4 ventral root. Scale bar = 50 μm. ***B,*** Higher magnification of the boxed region in panel ***A*** illustrating the dense network of motor neuron dendrites which extend dorsally in proximity to the pacemaker axon. Scale bar = 20 μm. ***C,*** Single optical section (0.5 μm) showing a higher magnification of boxed region in panel ***B***. Pacemaker axonal varicosities (*green*) are in close apposition to rhodamine-labeled motor neuron dendrites (*magenta*) in the deep dorsal horn of the neonatal spinal cord (*arrows*). Scale bar = 10 μm.

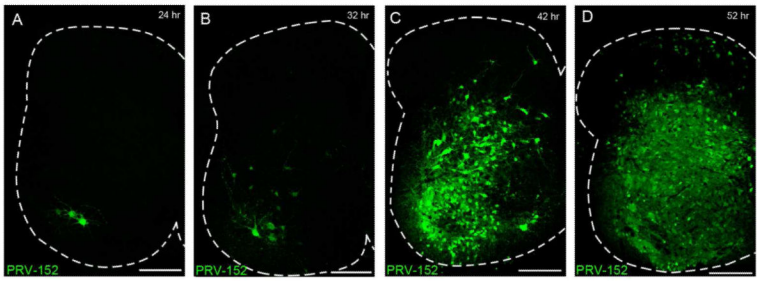

Figure 3.

Visualization of spinal motor pathways via the retrograde transport of PRV-152. ***A-D,*** Time course of PRV-152 labeling following injection into the left hindlimb quadriceps. Motor neurons are labeled beginning at 24 - 28 hours post-infection (p.i.) ***(A)***, with GFP expression appearing in premotor interneurons between 32 - 44 hours p.i. ***(B, C)***. ***D,*** At approximately 48 - 52 hours p.i., PRV-infected cells are clearly observed in the superficial dorsal horn. Scale bars = 200 μm.

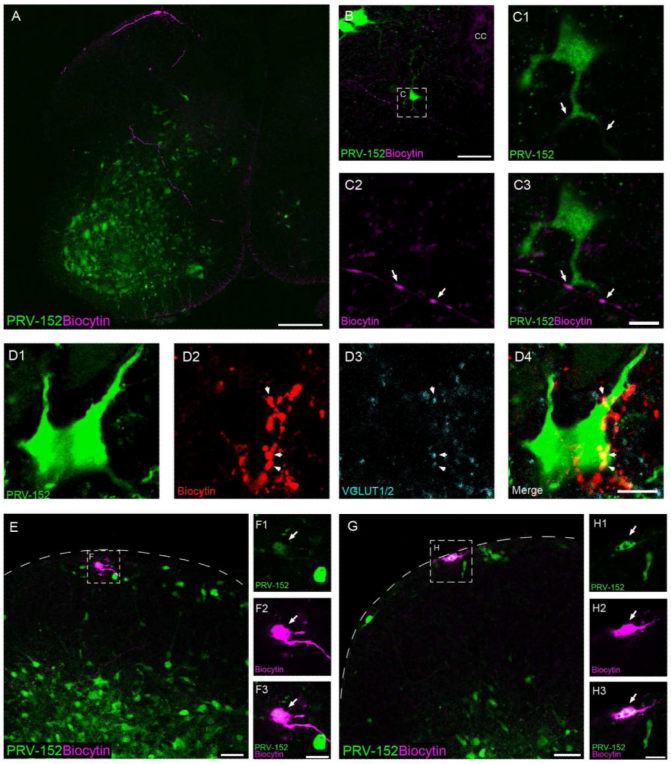

Figure 4.

Lamina I pacemakers synapse onto flexor motor pathways in the spinal cord. ***A,*** Example of a pacemaker axon (*magenta*) coursing through the deep dorsal horn and ventral horn of the neonatal spinal cord, where it lies in close proximity to numerous GFP-expressing cells following the injection of PRV-152 into the biceps femoris. Scale bar = 200 μm. ***B,*** Image depicting a pacemaker axon projecting towards the anterior commissure that makes putative contacts with the dendrites of a GFP-expressing cell in the ipsilateral ventral horn. CC = central canal; scale bar = 50 μm. ***C,*** Higher magnification of the boxed region in panel ***B***. Arrows indicate sites where the biocytin-filled axonal boutons (*magenta*) co-localized with GFP (*green*) in a single 0.5 μm optical section. Scale bar = 10 μm. ***D,*** Single optical sections (0.5 μm) illustrating an example of pacemaker axonal boutons (***D2***) positive for VGLUT1/2 immunoreactivity (***D3***) making putative contacts with a PRV-152 infected cell (***D1***) in the deep dorsal horn (***D4***). Scale bar = 10 μm. ***E-H,*** Examples of electrophysiologically identified lamina I pacemaker neurons that were infected with PRV-152 at 52 hours following virus injection into the biceps femoris, as evidenced by the co-localization **(*F3, H3*)** of biocytin labeling (***F2, H2****; magenta*) and GFP expression (***F1, H1*****;** *green*). Scale bars = 20 μm. ***F, H,*** Single optical sections (0.5 μm thickness) showing higher magnification of the boxed regions in panels ***E*** and ***G***, respectively. Scale bars = 10 μm.

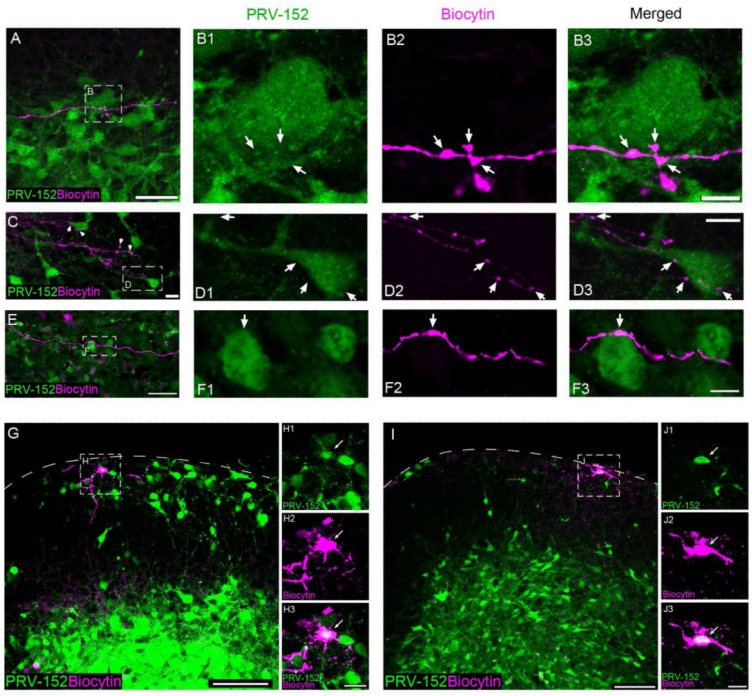

Figure 5.

Pacemakers engage spinal networks innervating hindlimb extensor muscles in the neonatal rat. ***A,*** Pacemaker axonal boutons (*magenta*) are in close apposition to a GFP-expressing soma (*green*) in the deep dorsal horn following PRV-152 injection into the quadriceps muscles. Scale bar = 50 μm. ***B,*** Single 0.5 μm optical sections showing higher magnification of the boxed region in panel ***A***, illustrating putative sites of contact between the pacemaker axon and the PRV-infected cell (*arrows*). Scale bar = 10 μm. ***C,*** A pacemaker axon branches extensively in the vicinity of numerous PRV-infected cells located in the deep dorsal horn. Scale bar = 20 μm. ***D,*** Higher magnification of the boxed region shown in ***C*** (single 0.5 μm optical sections) reveals multiple putative contacts between the axon of the pacemaker neuron and a GFP-expressing cell (*arrows*). Scale bar = 10 μm. ***E,*** Example of a pacemaker axon in close association with a PRV-infected soma in the spinal ventral horn. Scale bar = 50 μm. ***F,*** Single 0.5 μm optical sections showing higher magnification of the boxed region in ***E***. Scale bar = 10 μm. ***G-J,*** Examples of electrophysiologically identified lamina I pacemaker neurons that were infected with PRV-152 at 52 hours following virus injection into the left quadriceps, as evidenced by the co-localization ***(H3, J3)*** of biocytin labeling (***H2, J2****; magenta*) and GFP expression (***H1, J1*****;** *green*). Scale bars = 100 μm. ***H, J,*** Single optical sections (0.5 μm thickness) showing higher magnification of boxed regions in panels ***G*** and ***I***, respectively. Scale bars = 20 μm.

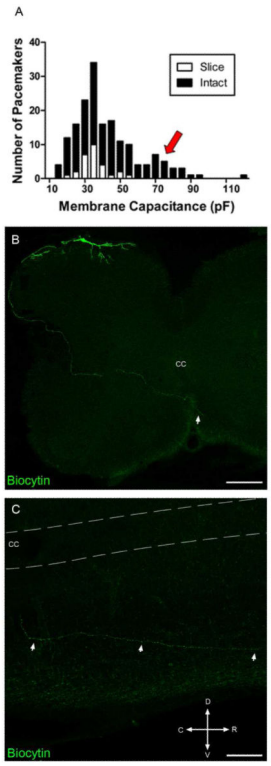

Figure 6.

The intact spinal cord contains a population of large pacemaker neurons with distinct axonal projection patterns. ***A,*** Histogram showing the distribution of pacemaker neurons as a function of membrane capacitance in the spinal cord slice (n = 28) vs. intact spinal cord preparations (n = 172). Arrow indicates a population of larger pacemakers identified in the intact spinal cord (*black*) which was not observed when recording from the spinal cord slice preparation (*white*; see also Li and Baccei 2011). ***B,*** Representative example of a large pacemaker neuron (recorded using the intact spinal cord preparation) whose axon projects to the contralateral side (*arrow*) via the anterior commissure. Composite images were constructed from 10 overlaid serial transverse sections (each 50 μm thick). Scale bar = 200 μm. ***C,*** Parasagittal section (50 μm) of the spinal cord on the side contralateral to the pacemaker soma, illustrating the rostral trajectory taken by the pacemaker axon after crossing the anterior commissure. CC = central canal; D = Dorsal; V = Ventral; R = Rostral; C = Caudal. Scale bar = 100 μm.

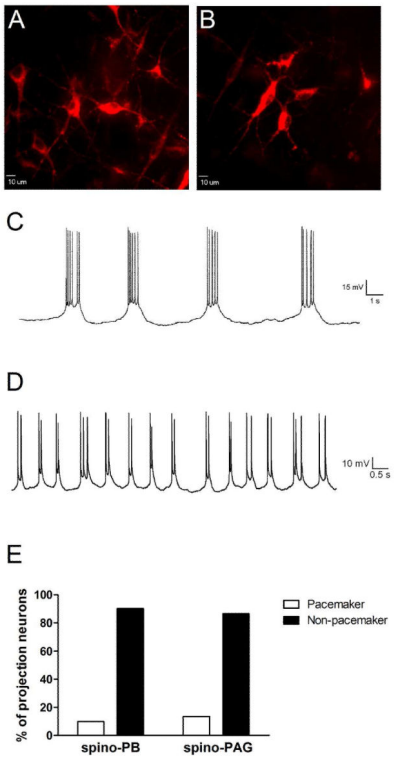

Figure 7.

Ascending lamina I projection neurons can exhibit pacemaker activity within the intact spinal cord network during early life. ***A, B,*** Representative confocal images of retrogradely-labeled lamina I projection neurons within the intact spinal cord preparation following DiI injection into the parabrachial nucleus (PB). Scale bars = 10 μm. ***C,*** Example of the rhythmic burst-firing which was observed in an identified spino-PB projection neuron during the neonatal period. ***D,*** A subset of pacemaker projection neurons exhibited shorter bursts of activity which were often characterized by spike doublets. ***E,*** There were no significant differences in the prevalence of pacemaker activity between the spino-PB (n = 41) and spino-PAG (n = 37) populations of projection neurons during the first postnatal week (p = 0.729; Fisher's exact test).

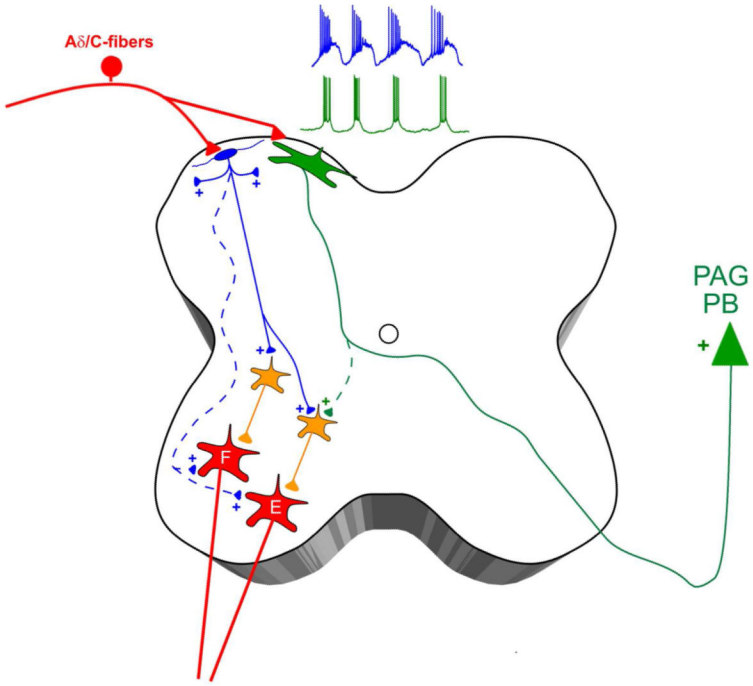

Figure 8.

Working model of pacemaker connectivity in the developing spinal cord. Lamina I of the neonatal dorsal horn is proposed to contain two distinct populations of pacemaker neurons, which are both innervated by high-threshold primary afferents (i.e. Aδ/C-fibers). Small pacemakers (*blue*) correspond to glutamatergic interneurons which project to the superficial laminae and/or to the deep dorsal and ventral horns, where they synapse onto premotor interneurons (*orange*) within flexor (F) and extensor (E) motor pathways. Meanwhile, the majority of large pacemakers (*green*) project their axons into the contralateral white matter and correspond to ascending projection neurons targeting supraspinal sites of nociceptive processing such as the parabrachial nucleus (PB) and periaqueductal gray (PAG). Dotted lines represent potential synaptic connections which require further investigation.

Table 1

Antibodies Used in Study

Primary Antibodies

Antibody Name	Immunogen	Manufacturer, catalog, RRID, host	Dilution
Living Colors® Full-length GFP Polyclonal Antibody	Recombinant full-length *Aequorea coerulescens* green fluorescent protein (aAcGFP1).	Clontech Laboratories Inc., 632592, AB_2336883, rabbit, polyclonal	1:1000
Anti-Vesicular Glutamate Transporter 1 (VGLUT1)	Synthetic linear peptide from rat VGLUT1 protein (C-Terminus; amino acids 456-560)	Millipore, AB5905, AB_2301751, guinea pig, polyclonal	1:3000
Anti-Vesicular Glutamate Transporter 2 (VGLUT2)	Recombinant GST-tagged protein (amino acids 565-582; VQESAQDAYSYKDRDDYS)	Millipore, AB2251, AB_1587626, guinea pig, polyclonal	1:5000

Secondary Antibodies

Antibody Name	Manufacturer, catalog RRID, host	Dilution
Anti-guinea pig IgG (H+L), highly cross-adsorbed conjugated to AlexaFluor 488, 594, 647	Invitrogen (Molecular Probes), A11703 AB_2307359, A11076 AB_2307360, A21450 AB_141882, goat	1:1000
Anti-rabbit IgG (H+L) conjugated to AlexaFluor 488	Invitrogen (Molecular Probes), A11008 AB_143165, goat	1:1000